



Evaluation of antibacterial activity, in-vitro cytotoxicity and catalytic activity of biologically synthesized silver nanoparticles using leaf extracts of *Leea macrophylla*

Shamsad Sharmin^a, Md Badrul Islam^a, Barun Kanti Saha^a, Firoz Ahmed^a,
Bijoy Maitra^a, M. Zia Uddin Rasel^a, Nazeeb Quaisar^b, M. Ahasanur Rabbi^{a,*}

^a BCSIR Laboratories Rajshahi, Bangladesh Council of Scientific and Industrial Research (BCSIR), Rajshahi, 6205, Bangladesh

^b Department of Civil Engineering, Rajshahi University of Engineering & Technology (RUET), Rajshahi, Bangladesh

ARTICLE INFO

Keywords:

Leea macrophylla
Silver nanoparticles
Biosynthesis
Antibacterial activity
Cytotoxicity
Catalytic activity

ABSTRACT

Nanotechnology has become a cutting-edge field of research that has emerged as an interdisciplinary research area and contributes to almost every field of science. With the increasing demand for sustainable greener products, attention has recently been focused on green nanotechnology. This study manifested the aptitude of *Leea macrophylla* (LM) leaf extract, fortified with phytochemicals, to biosynthesize silver nanoparticles (AgNPs) for the first time. As soon as the AgNPs were biosynthesized, they immediately changed color, and the distinctive surface plasmon resonance (SPR) occurred at 420 nm in the Ultraviolet-Visible spectrum, proving that the biosynthesis had been successful. Fourier Transform Infrared Spectroscopy (FTIR) was used to examine the phytochemicals present in the LM leaf extract, those are accountable for the formation and stabilization of AgNPs. The Transmission Electron Microscope (TEM) revealed the formation of quasi spherical silver nanoparticles with an average diameter of 22.77 nm. Synthesized nanoparticles were further characterized by X-ray diffraction (XRD), Field Emission Scanning Electron microscope (FESEM), Energy Dispersive X-ray (EDX), Dynamic Light Scattering (DLS) and Thermogravimetric analysis (TGA). The production of AgNPs with high metal content from LM leaf extract exhibited encouraging results. The LM leaf extract mediated silver nanoparticles evinced significant antibacterial and catalytic activities. The cytotoxicity effects of biosynthesized AgNPs were tested on brine shrimps.

1. Introduction

Scientists value the biosynthesis of nanoparticles due to the ability to use plant extracts as both bio reducers and capping agents [1–4]. This approach has significantly altered the traditional method of nanomaterial synthesis, which relied primarily on chemical routes [5,6]. The biosynthesis technique's simplicity and biocompatibility have appealed to researchers for years, making it a sustainable and cost-effective option for nanoparticle synthesis. Nanostructures exhibit unique chemical and electrical properties, not present in their bulk counterparts [7–9]. Recent advancements in devices, operated at the nanometer scale have demonstrated the ability to lead to new applications in fields such as nanoscale electronics, catalysis, bio-nanomedicine, and photo-electrochemical

* Corresponding author.

E-mail addresses: rabbi_chem@yahoo.com, ahasanurrabbi@bcsir.gov.bd (M.A. Rabbi).

<https://doi.org/10.1016/j.heliyon.2023.e20810>

Received 22 June 2023; Received in revised form 4 October 2023; Accepted 6 October 2023

Available online 7 October 2023

2405-8440/© 2023 The Authors. Published by Elsevier Ltd. This is an open access article under the CC BY-NC-ND license (<http://creativecommons.org/licenses/by-nc-nd/4.0/>).

applications [10,11]. Several elements falling in the noble metals category including silver, gold, palladium, and copper, have been utilized to create nanoparticles [12]. Among them, silver nanoparticles have demonstrated effectiveness in cancer diagnosis and treatment, as well as antibacterial and catalytic agents [13,14]. Distinctive approaches, comprising chemical reduction, micro emulsions, hybrid methods, photochemical reduction, sonoelectrochemical, and microwave-based systems, have been developed for the production of silver nanoparticles [10,15]. Growing metal nanoparticles in a green manner, with the help of plants, has gained a lot of attention over the past few years. This is because traditional methods of synthesizing these materials, such as chemical reduction or microemulsions, often rely on hazardous chemicals or are prohibitively expensive [6,15]. Green synthesis techniques, on the other hand, offer a safer and more sustainable alternative. These methods utilize naturally occurring reducing and capping agents found in plant extracts, sugars, biodegradable polymers, and microbes to produce nanoparticles [16,17]. Plant extracts have emerged as a popular choice and preferred over microorganisms, taking into consideration their low toxicity and cost-effectiveness, and no requirement of a long-term collection of microbial cultures [7]. Researchers have found that green synthesis techniques are often simpler, one-step processes that can be easily repeated, resulting in a more consistent product. Those concerned with environmental and biological impacts are encouraged to consider green synthesis using plant extracts as a viable option.

Particularly in the green production of AgNPs, silver salt solutions like AgNO_3 are reduced utilizing plant extract. In the first phase, known as the nucleation phase, silver atoms use high activation energy to form tiny nuclei; in the second, known as the development phase, these tiny nuclei bond together to produce nanoparticles (NPs). When stable particles in aqueous solutions devoid of stabilizers are created from the AgNPs, the reduction potential of the Ag metal drastically increases [8]. Reduced Ag is toxic to microbial life because it ruins cell membranes and interferes with their metabolic activities and development [7]. Therefore the literature survey showed that AgNPs have potential antimicrobial activities against various microorganisms [15]. Antioxidant action is imparted onto plant derived AgNPs by the surface coating of plant biochemical compounds [18]. Antifungal, anti-inflammatory, antiviral, anti-angiogenesis, antiplatelet, and anticancer properties have also been found for AgNPs [19]. Sensors, spectroscopy, electronics, and many more have all made use of silver nanoparticles (AgNPs) [20].

We present here a method for green synthesis of silver nanoparticles using *Leea macrophylla* (LM) leaf extract as a pristine substitute. *Leea macrophylla*, also known as Hastikarna Palash, is a plant found in various regions of Bangladesh, including Natore, Rajshahi, Dinajpur, Savar, and the Chittagong hill area [21,22]. It belongs to the Leeaceae family and is characterized by its large leaves that resemble elephant ears. LM is an herb or herbaceous shrub with a large leaf that resembles the ear of an elephant. The leaves are simple and can reach up to 60 cm in length, while the roots are tuberous and perennial [23]. Treatment for guinea worm, ringworm, boils, arthritis, gout, rheumatism, stomach tumours, lipoma, tetanus, tonsillitis, sores, soreness, blood effusion, ischemic disorders, and other conditions have all been reported to improve after using this plant [22,24–26]. Furthermore, pharmacological studies on LM were conducted, revealing its anti-inflammatory, antiurolithiatic, antinociceptive, cytotoxic, analgesic, antimicrobial, hepatoprotective, anti-amnesic, neuroprotective, and antioxidant properties [27,28]. During phytochemical research, leaf extracts were found to contain alkaloids, glycosides, steroids, reducing sugars, and so on [23]. Additionally, phenolics and flavonoids were found in the leaf extract, which will be studied in this research to investigate whether these secondary metabolites can be used as reducing or capping agents in the production of AgNPs and their various functions.

2. Experimental

2.1. Materials

The leaves of the plant *Leea macrophylla* were plucked from the Bangladesh Council of Scientific and Industrial Research's Garden in Rajshahi, Bangladesh. The experiment only employed chemicals of sufficient purity to serve as reagents. Sodium hydroxide (NaOH) was acquired from Merck, Germany, while silver nitrate (AgNO_3) was procured from Merck, India. All the bacteria were fetched from International Centre for Diarrhoeal Disease Research, (icddr,b) Dhaka, Bangladesh before preparing microbial cultures in Chemistry Laboratory, Rajshahi University, Rajshahi, Bangladesh. Brine Shrimp (*Artemia salina*) eggs had been procured from local market, Kolabagan, Dhaka, Bangladesh.



Fig. 1. *Leea macrophylla* tree and its leaf.

2.2. Preparation of *Leea macrophylla* leaf extract

The green LM leaves (Fig. 1) were thoroughly cleansed with distilled water to remove the dust and silt on the leaves. After that, the leaves were minced into little pieces. 160 g of chopped leaves were combined with 1000 mL of distilled water to create the plant extract. This mixture received 10 mL of 1 M NaOH, which was then agitated for an hour at 55 °C. A clear brown color developed after the liquid portion of the plant was collected and repeatedly filtered using Whatman no. 1 filter paper.

2.3. Biosynthesis of LM-AgNPs

De-ionized water was used to make a 0.01 M concentration of AgNO₃. A 100 mL solution of clear brown extract of LM leaf was combined with 10 mL of 1 M NaOH solution and agitated for 5 min. 200 mL AgNO₃ solution was added slowly and continuously swirled at 500 rpm. The reaction involved purging inert N₂ gas through the reaction vessel which was under airtight condition. The entire process was operated at room temperature (25 °C) and stirring continued for 6 h. The reaction mixture was left to stand in the dark for 12 h. After 12 h the reaction vessel was taken out from the dark room and centrifuged at 9000 rpm using SIGMA Laboratory Centrifuges. The supernatant liquid was drawn off and the sediment redispersed in de-ionized water before being centrifuged for second time. This process was repeated until the supernatant became neutral. Finally, the dispersion of *Leea macrophylla* leaf extract mediated silver nanoparticles (LM-AgNPs) was collected in a screw cap bottle and stored.

2.4. Characterization of AgNPs

Following synthesis of silver nanoparticles, assessment on their optical properties was accomplished using UV-visible spectrophotometer (UV-Vis-NIR-3600i Plus spectrophotometer, Shimadzu). This procedure enabled us to obtain the absorption peak at lambda max (λ_{max}) for both LM leaves extract solution and LM-AgNPs dispersion. For the Fourier transform infrared spectroscopy (FTIR) spectrum analysis, the biosynthesized silver nanoparticles powder was powdered with KBr pellet in mortar and pestle and FTIR spectrum of synthesized recorded by FTIR-ATR Spectrum two (PerkinElmer, UK). For comparison, LM leaf extract was dried and FTIR spectrum recorded in the same manner. With an average of 20 scans, the spectra were measured between 400 cm⁻¹ and 4000 cm⁻¹. Scanning X-ray diffractometer (Bruker D8 Advance, Germany) was used to record the X-ray diffraction (XRD) patterns of the synthesized LM-AgNPs where the intensity measurement was done at 2 θ values from 10 to 80° with scanning rate 1° min⁻¹ at 25 °C. It was possible to minimize noises, smooth the data, and pinpoint peaks by integrating the diffraction spectrum with a position-sensitive detector aperture utilizing semi-quantitative phase analysis programs. Thermal stability of LM-AgNPs was monitored utilizing PerkinElmer Simultaneous Thermal Analyzer STA 8000, PerkinElmer, Netherland. The weight loss percentage was measured after drying about 10 mg of the dry powdered sample within constant circulating nitrogen environment at a heating rate of 20 °C min⁻¹.

All SEM images were captured with a JSM-7610F Field Emission Scanning Electron Microscope, operating in the range of 5–15 kV, while magnifying images up to 200,000 \times . JEOL Auto fine coater (JEC-3000FC) sputtered platinum coating to the dried sample prior to SEM imaging. Energy dispersive X-ray spectroscopy adapter connected to SEM was used for collecting the EDX spectra. To investigate the size and shape of synthesized LM-AgNPs transmission electron microscope (TEM) images were taken by Talos F 200X, ThermoFisher Scientific. During TEM measurement, a 300-mesh copper (Cu) grid was covered in carbon film. A little amount of sample solution was then dropped to the grid, and the solvent was subsequently evaporated at room temperature in presence of air. The particle size analyzer was used to look at the size distribution and polydispersity index (PI) of the generated LM-AgNPs. In this case, a Horiba analyzer (SZ-100) was used to examine the NPs' colloidal dispersion. At 25 °C and a scattering angle of 90°, dynamic light scattering (DLS) can determine the size of particles.

2.5. Antibacterial activity assay

This study was carried out using disk diffusion assay method [29,30]. The silver nanoparticle that is prepared with *L. macrophylla* leaf extract were investigated for antibacterial efficacy on six bacteria (2 Gram positive: *Bacillus cereus*, *Staphylococcus aureus*; 4 Gram negative: *Pseudomonas taiwanensis*, *Pseudomonas monteilii*, *Kosakonia oryziphila*, *Mangrovibacter yixingensis*) at three different concentrations of LM-AgNPs (40, 60, 80 μ g/disk) along with a standard antibiotic, *Kanamycin* (30 μ g/disk). Optimizing growth conditions of bacteria strains, these 6 strains were grown overnight in nutrient broth that were placed in a shaker at 35 °C temperature and 120 rpm for antibacterial activity evaluation. 1 mL of overnight culture was transferred and gently spread on the nutrient agar plate and dried. Antibiotic disk, along with 3 separate disks containing LM-AgNPs with varied concentrations samples shown in figure were placed on the respective plates (4 disks per plate) and incubated overnight at 35 °C. After incubating overnight at 37 °C, the diameters of the clear-zones in millimeters were considered to determine the LM-AgNPs' ability in combating the tested bacteria. Each experiment was performed three times, averaging the diameters of the inhibitory zones around each filter paper disk.

2.6. Cytotoxicity assay

The Meyer et al. simplified approach for determining the Brine shrimp lethality test was implemented in this study [31]. The cytotoxicity test was run with *A. salina* eggs (cysts) as the yield from hatching these organisms was high. The eggs were convenient to collect from the aquarium pet store. Within a salt solution (2–4%) made out of pond water with table salt, larvae (nauplii) develop from shrimp eggs. The cysts absorbed water and hatched within 24 h. The freshly hatched nauplii were transferred to different

concentrations (10, 20, 30, 40, 50 μL) of LM-AgNPs and left untouched for 24 h. To quantify the cytotoxicity level of LM-AgNPs, the number of surviving nauplii in each test tube after 24 h was noted. Each experiment was repeated three times, and the findings were averaged. Percentage mortality [32] was figured out by following the formula:

$$\% \text{Mortality} = \frac{\text{Number of dead } Artemia \text{ nauplii}}{\text{Initial number of living } Artemia \text{ nauplii}} \times 100$$

2.7. Catalytic activity

Aqueous solution of Congo Red (CR) dye was degraded by LM-AgNPs and their catalytic activity was evaluated in the presence of NaBH_4 . 5.0 and 10 $\mu\text{g}/\text{mL}$ of LM-AgNPs was added to a solution of 18 mL of 0.1 mM CR dye and 1 M NaBH_4 (2.0 mL). Absorbance at a constant wavelength of 500 nm was measured to track the time-dependent decrease in CR concentration in aqueous solution. The experiment was repeated without the catalysts to serve as a control.

3. Results and Discussions

Phytoconstituents in *Leea macrophylla* leaf extract brought about the conversion of Ag^+ ions to metallic Ag [33]. The outcome of biosynthesis, i.e., bio-reduction of silver nanoparticles from silver ions, was visually distinguished by the distinct shift in color that resulted during the one-pot synthesis. Light brown colored LM leaf extract adjusted to brownish-black colored solution upon addition of colorless silver nitrate solution, which was then stabilized to give a dark brown end reaction mixture (Fig. 2). Surface plasmon resonance phenomenon can be accountable for this activity [34]. In our work, disruption of natural eco-cycle was avoided by not applying external high energy, temperature, or harmful chemicals as reducing and stabilizing agent. For this successful green synthesis, reaction parameters were suitably modified.

Fig. 3 shows the UV-vis absorption spectrum of the synthesized silver nanoparticles. UV-visible spectroscopy is a popular method for nanoparticles investigation and silver nanoparticles' free electrons cause surface Plasmon resonance (SPR). The absorption peak (SPR) of the synthesized LM-AgNPs was observed in the visible range and to be centered at 420 nm. This specific SPR is a characteristic band for the Ag [35,36]. There are no peaks located in this region, indicating the formation of pure silver nanoparticles. The study was carried out for a three-month period to check for the stability and no big difference was found in the peak position.

FTIR was adopted to investigate the naturally occurring substituent incorporated in the produced LM-AgNPs. Fig. 4 shows the FTIR spectra of LM leaf extract and synthesized silver nanoparticles (LM-AgNPs). With the exception of a little alteration in peak location and intensity, the FTIR spectra of LM-AgNPs (Fig. 4b) was quite comparable to that of the leaf extract (Fig. 4a). Both spectra were discovered to have broadening bands at 3600-3200 cm^{-1} due to the stretching vibrations of O-H (alcohol/phenol). In FTIR spectrum of LM leaf extract (Fig. 4a) the O-H stretching vibrations give a broad and intense absorption band compared to LM-AgNPs [37]. High amount of hydrogen bonding was responsible for this broad and strong absorption peak, whereas the formation of nanoparticles decreases the hydrogen bonding as well as free hydroxyl group. Also, N-H group could be present [38]. Observing fluctuation in peaks from 3388 to 3259 cm^{-1} , participation of the functional groups mentioned above in synthesis of silver nanoparticles became obvious [39]. The absorption peak at 1600 cm^{-1} was deemed to be due to the C=C and C=O stretching [40,41]. This absorption band change to 1637 cm^{-1} , which is weaker in intensity than that of 1600 cm^{-1} , was detected in vibrational modes of organic compounds as LM-AgNPs were formed, highlighting possible contribution of biomolecules in this synthesis.

Moreover, bands at 3388 and 1600 cm^{-1} in LM leaf extract might be reflected to exist due to N-H bond and carbonyl stretching frequency of amide linkage or flavonoids present in the extract [42,43]. These biomolecules, hence, assist in forming and binding AgNPs. The peak at 1406 cm^{-1} in leaf extract was thought to originate from C-H bending in alkane, N-O stretching, and C-N stretching, and for bioreduced silver nanoparticles this band relocated at 1427 cm^{-1} . In the FTIR spectrum of LM leaf extract a peak at 1071 cm^{-1} was found due to C-O stretching [39]. The disappearance of this band in prepared LM-AgNPs could be because of leaf phytoconstituents actively participating in reduction and stabilization of silver nanoparticles. Infrared spectrum can give a high ground in deducing the constitutional functional groups associated to infrared absorptions observed [44]. Thus, this inspection helps to figure out the functional groups that have the inclination to reduce silver ions and wrap up the bio-reduced LM-AgNPs. It was reported that the extract of LM leaves was rich in phenolic and flavonoid contents and the compounds had been spotted in methanol extract of *Leea macrophylla* by GC-MS [45].

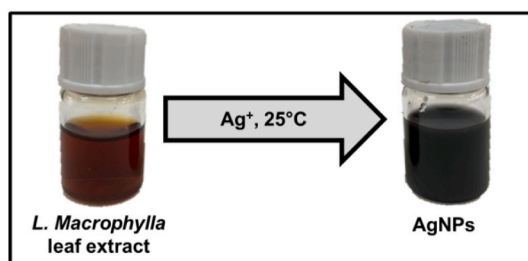


Fig. 2. Color change due to the formation of LM-AgNPs

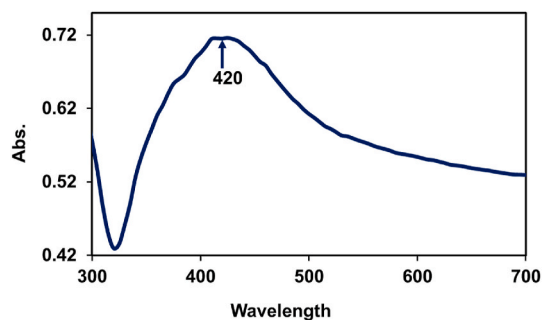


Fig. 3. UV-Vis spectrum of LM-AgNPs.

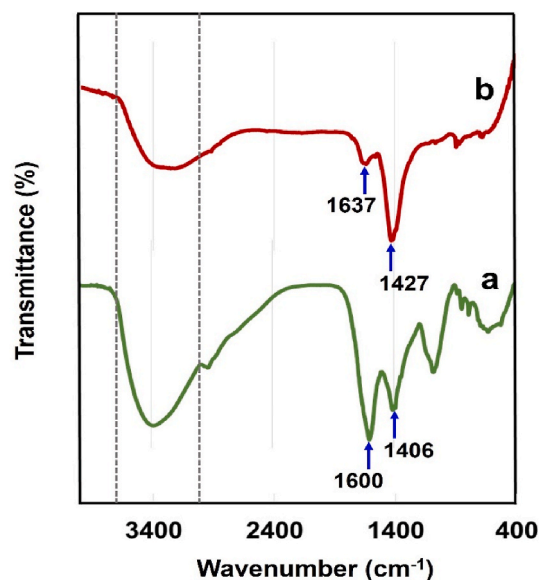


Fig. 4. FTIR spectra of (a) LM leaf extract and (b) LM-AgNPs.

The thermal stability of synthesized LM-AgNPs was investigated using thermogravimetric analysis (TGA). TGA helps to confirm the existence of biomolecules in LM-AgNPs. In this method high temperature (800 °C) was uniformly raised from room temperature and the weight loss was calculated against it; eventually this had plotted in graph for examining purpose (Fig. 5). The curve showed a loss of mass of about 1.3% at the very beginning at a temperature over a range of temperature from around 30 °C–285 °C, largely due to the removal of water content of the sample [46]. As the excess of the organic compounds of the leaf extract capping AgNPs burnt out, the weight% further declined over the temperature range of about 290 °C–350 °C [47]. The weight stabilized from around 350 °C and steadied as the temperature rose to 800 °C. There was no further weight loss up to 800 °C, and at that temperature, 97.3% of the

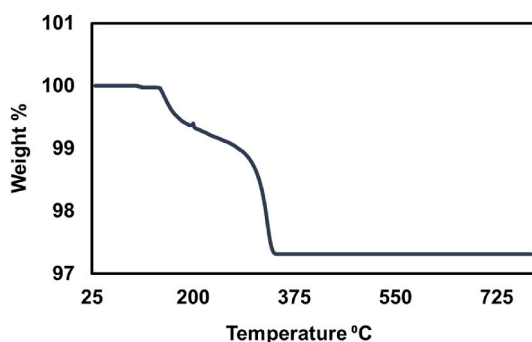


Fig. 5. TGA diagram of biosynthesized LM-AgNPs.

original mass was still there. As a result, the particles' residual mass (~97 %) was explained by the existence of LM-AgNPs' high metallic content.

Diffraction beam intensities with their associated atomic positions of silver nanoparticles prepared with LM leaf extract were recorded using X-ray diffractometry. The crystalline nanoparticles of silver could be verified by looking at the plane-indexed peaks of the diffraction pattern in Fig. 6. Peaks occurring at 38.18° , 44.31° , 64.55° , 77.45° and their indices of the satisfied planes (111), (200), (220) and (311) had been ensued, accentuating formation of face-centered Ag [JCPDS number: 04-0783]. Not common among the aforementioned answerable metal nanoparticles' peaks, there also was a crystalline band at 33.22° that suggested more activity of silver ions being broken down to metallic silver, thus encouraging enhanced biomolecular-reduction of the leaf extract. The highest intensity peak resulted when the Bragg diffraction condition was fulfilled by the crystallographic (111) plane. With FWHM of (111) diffraction peak following Scherrer's formula the mean grain size of the as-prepared LM-AgNPs was identified in nano-sized range.

Fig. 7i portrayed Field emission scanning electron microscope (FESEM) of the synthesized LM-AgNPs. The morphology of the LM-AgNPs was determined by FESEM and from the images, the spherical morphology of silver nanoparticles is randomly distributed with average diameter <50 nm. The concentrated nanoparticles interact with the phytochemicals of LM leaf extract contributing to synthesis, causing the particles to agglomerate in layers [48]. Solvent evaporation, while nanoparticle film was preparing for FESEM imaging, generated minor clusters of nanoparticles. Clustering of nanoparticles may also arise due to cross linking between the stabilizing agents; this similar result was discussed by Ref. [49]. Despite of such aggregation individual particles size and shape of LM-AgNPs can be identified from the FESEM images. Almost all particles were spherical or quasi spherical. Transmission electron microscope (TEM) images also confirmed the formation of LM leaf extract mediated silver nanoparticles. Particle images with varying degrees of contrast reveal the presence of organic phytochemicals in LM leaf extract [48]. As evident in Fig. 7(ii), a preponderance of spherically embossed silver nanoparticles was characterized by the photographed TEM images occupying many nanoparticles. The amount of time the electron beam was exposed to the specimen and time spent treating the specimen likely provided nanoparticles with a chance to agglomerate [50]. While the sample was being prepared, the slow loss of water pushed the particles closer together, and the formation of aggregates was sped up by the hydrogen bonds that formed between the biomolecules presented as capping agents [50]. However, despite aggregation, some discrete particles smaller than 100 nm are still discernible (pointed by yellow lines). Fig. 7 (iii) displays a quite narrow distribution, with most particles falling between 10 and 30 nm in size, while the average diameter of LM-AgNPs was 22 nm.

The average hydrodynamic diameter of the generated LM-AgNPs colloidal dispersion, as determined by the DLS histogram, was around 296.1 nm (Fig. 8). DLS doesn't measure the actual size of the nanoparticles; instead, it measures the diameter of the particles as they are disseminated in liquid. DLS results in this study for biosynthesized LM-AgNPs are, consequently, larger than those obtained by SEM and TEM. According to the report [51–53], the difference in size between DLS and SEM and TEM results from the influence of Brownian motion. Mulvaney (1996) [54] stated that "good" colloidal solutions are those with a polydispersity index (PI) value lower than 0.50. Despite partial aggregation, the size of some individual particle or clusters of LM-AgNPs were still below 100 nm (yellow color line in TEM image) and the PI for the colloidal dispersion of LM-AgNPs was 0.411. AgNPs produced by a biosynthesis process driven by LM leaf extract create a nearly monodisperse colloidal dispersion. According to results previously reported for colloidal nanoparticle stability, the dispersion was confirmed to be stable [55].

EDX spectrometers revealed the elemental silver signal for the existence of silver nanoparticles (Fig. 9). The energy dispersive analysis of x-rays (EDX) revealed at 2.983 keV silver nanoparticles was substantiated due to noteworthy intense peak of silver nanoparticles. Surface Plasmon resonance [56] has been responsible for such sharp peak. From these data we can see that peaks are due to the existence of elements such as Ag, O, C; additionally, no peak had been registered that symbolized no existence of impurities. The weight percentage (W%) of silver was found to be 89.31 %, whereas the weight percentage (W%) of oxygen and carbon were found to be 6.77 % and 3.92 %. The high metal content was in good agreement with TGA result.

The antibacterial activity of LM-AgNPs was assessed using the disk diffusion method. Over the last decade, antibacterial activity of silver nanoparticles has been investigated by many researchers and extensive documentation on the antibacterial properties of silver nanoparticles has been carried out by several workers. It's worth mentioning that previous investigations of antibacterial capabilities shown a wide range of fluctuation. Due to the fact that there is no universally accepted means for determining the antibacterial activity of AgNPs, it is challenging to draw meaningful comparisons between the findings [57]. Moreover, researchers have used a variety of

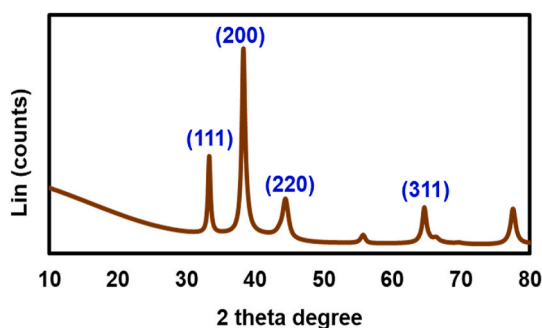


Fig. 6. XRD pattern of LM-AgNPs.

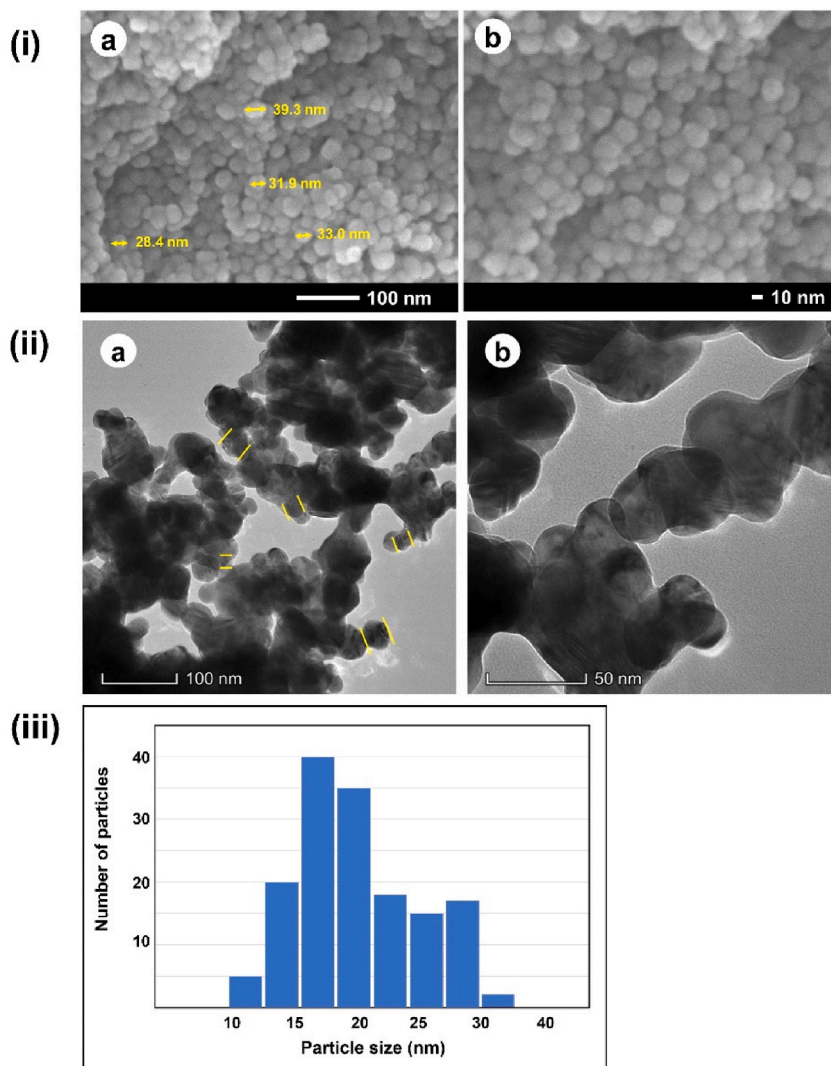


Fig. 7. (i) FESEM images of LM-AgNPs at (a) low and (b) high magnifications; (ii) TEM images of LM-AgNPs at (a) low and (b) high magnifications; (iii) Particle size distribution histogram.

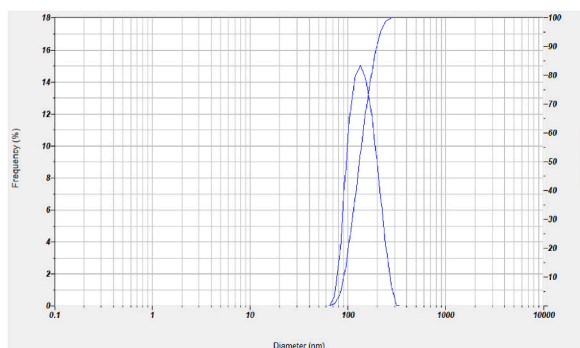


Fig. 8. Size distribution of LM-AgNPs as studied by DLS.

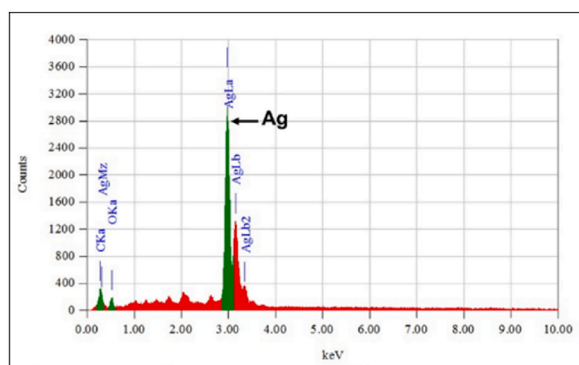


Fig. 9. EDX spectra of LM-AgNPs.

approaches. In this study the prepared LM-AgNPs were found to be active against both gram-positive and gram-negative bacteria. The antibacterial activity of LM-AgNPs showed significant positive activity in dose-dependent manner. Fig. 10 represents the antibacterial activity of LM-AgNPs with three different concentrations against six pathogens. The maximum activity was found for 80 $\mu\text{g}/\text{disk}$ LM-AgNPs against *B. cereus*. With the maximum dose (80 $\mu\text{g}/\text{disk}$) LM-AgNPs showed the inhibition zones 16.0, 20.0, 16.0, 17.0, 16.0, and 17.0 mm against *S. aureus*, *B. cereus*, *P. taiwanensis*, *P. monteilii*, *K. oryziphila*, and *M. yixingensis* respectively. The outcome implies that the synthesized LM-AgNPs showed similar and in some cases higher inhibition effect than that of reference antibiotics Kanamycin (30 $\mu\text{g}/\text{disk}$). It is still vague to understand the actual cause that leads to antimicrobial activity of AgNPs on microorganisms. According to Raghavendra et al., bacterial cellular destruction is caused by nanosized silver particles invading the cell wall and causing the plasma membrane to rupture [58]. In this study, high antibacterial activity of synthesized LM-AgNPs can be explained simply by the higher amount metal content in the synthesized particles. The existence of higher amount of silver content was also supported by TGA and EDX analysis of the LM-AgNPs.

Plenty of research on ecotoxicology experiments for nanomaterials have been conducted employing bacteria [59], fish larvae [60] and many other organisms. There is evidence that artemia is extremely toxic-sensitive in its early phases of development [61,62]. This research also demonstrates the viability of assessing the ecotoxicity of nanoparticles using the brine shrimp (*A. salina*) nauplii (Fig. 11). For frequent demands of toxicity screening [63], for potential and easy-to-use pharmacological activity [64], for cheaper availability [65] artemia-based toxicity assays of NPs are a key solution. In the standard Artemia test, freshly hatched *A. salina* larvae were exposed to LM-AgNPs suspensions. The percentage of mortality and toxic consequences were presented as LC₅₀. The parameters for toxicity were selected to be the concentration of a substance at which half of the tested animals die after 24 h [66]. The primary biotic cause of naupliar death could be identified as high content of LM-AgNPs building up in their body within 24 h after exposure [66]. Control cases had an insignificantly low mortality rate (about 3 %). Even at the lowest dose of 20 $\mu\text{g}/\text{mL}$, there was a mortality rate of about 28.3 %; however, as concentration raised to 40 $\mu\text{g}/\text{mL}$, 60 $\mu\text{g}/\text{mL}$, 80 $\mu\text{g}/\text{mL}$, death increased to about 36.6 %, 51.6 %, 65 %, which grew further, reaching a peak of 80 % at 100 $\mu\text{g}/\text{mL}$. At 24 h the LC₅₀ value was found around 60 $\mu\text{g}/\text{mL}$ of concentration [32,66,67]. Moreover, high mortality did occur from prolonged exposure over the next 48 h. Almost two times as many nauplii died after 48 h as did so after 24 h. The lowest dose of 20 $\mu\text{g}/\text{mL}$ show mortality of about 58.3 %. As concentration further spanned between 40 $\mu\text{g}/\text{mL}$, 60 $\mu\text{g}/\text{mL}$, 80 $\mu\text{g}/\text{mL}$, and 100 $\mu\text{g}/\text{mL}$ the mortality increased to 76.6 %, 86.6 %, 90 % and 93.3 % respectively. Larvae were subjected to starvation, while they are getting full with LM-AgNPs sediments. The results of the brine shrimp lethality assay (BSLA) clearly shows that at higher LM-AgNPs concentrations the number of living shrimp larvae was in lesser amount than that at lower concentrations. Additionally, as the concentration of the silver nanoparticles increased, the cytotoxicity also increased, which led to a decrease in the number of shrimp larvae that were still alive after 24 h.

In third world countries like Bangladesh, India and Pakistan the industrial wastewater discharged after improper treatment or in some cases without treatment [68]. Such wastewater containing synthetic dyes and other harmful chemicals is detrimental for the environment and living beings. To protect the environment, dye wastewater should have adequate treatment to avoid potentially disastrous consequences of the dyes. Conventional methods of water purification often struggle to eradicate these contaminants. Although there are various methods which are used for waste water treatment, there are drawbacks to almost all of these approaches, such as their high price label, their potential to produce secondary pollutants, their lack of efficiency, their complicated nature, and so on. Effluent treatment systems need to be improved as a result [69]. In this study, a model azo dye (Congo red) degradation potential of biosynthesized LM-AgNPs along with sodium borohydride (NaBH_4) was investigated. Congo Red (CR) dye was eliminated from water medium by catalytic reduction. This was done in the presence of different amounts (5.0 and 10.0 $\mu\text{g}/\text{mL}$) of LM-AgNPs catalyst. Fig. 12 depicts the reductive degradation of CR dye with the addition of LM-AgNPs catalyst at varying quantities (5.0 and 10.0 $\mu\text{g}/\text{mL}$). After the addition of LM-AgNPs catalyst, degradation of dye was visually observed within a few minutes by the change of deep red color, which was further confirmed by the decrease in absorbance value. The azo dye was completely degraded within 5 and 7 min in presence of 5.0 and 10.0 $\mu\text{g}/\text{mL}$ LM-AgNPs catalyst respectively. As with any catalyst system, the degradation rate increased with increasing catalyst concentration. The catalytic activity of nanoparticles is mainly dependent on the total surface area of the particles. The degradation rate of CR using LM-AgNPs is quite fast. This fast degradation can be explained by the high silver content within the

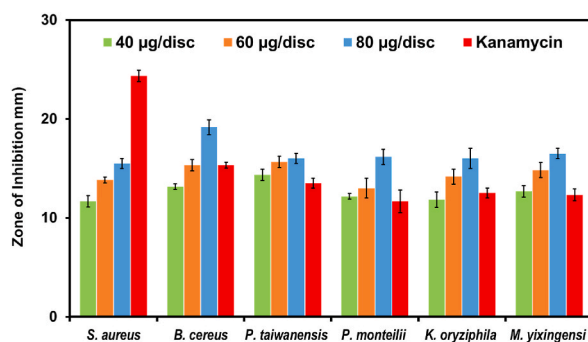


Fig. 10. Antibacterial activity of LM-AgNPs.

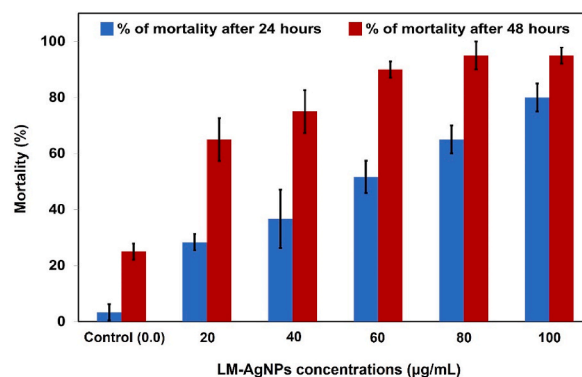


Fig. 11. Bar diagram displays outcome for the mortality rate (24 and 48 h) of brine shrimp *Artemia nauplii* exposed to different concentrations of silver nanoparticles.

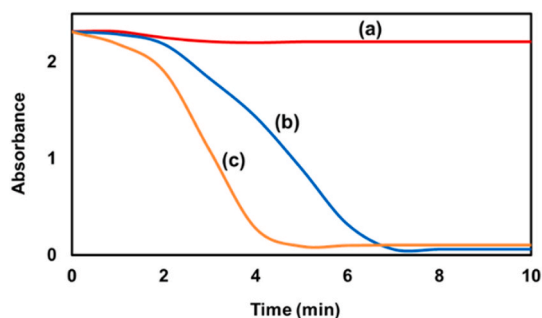


Fig. 12. Reductive degradation of CR dye solution in presence of (a) no catalyst, (b) 5 µg/mL and (c) 10 µg/mL LM-AgNPs catalyst.

synthesized nanoparticles, which is in agreement with the previous study reporting on the catalytic activities of AgNPs and AgNPs based nanocomposite [50].

4. Conclusions

This present research focuses on an aqueous leaf extract of a perennial plant locally known as Hathikana (*Leea macrophylla*), to create silver nanoparticles in a sustainable way. *Leea macrophylla* leaf extract mediated silver nanoparticles abbreviated as LM-AgNPs were successfully prepared through a simple one pot synthesis and this is the first report of biosynthesis of AgNPs using the leaf extract. Synthesis was ascertained to be cost effective and efficient in terms of reaction conditions (time and temperature). Moreover, synthesized LM-AgNPs were found to be quite stable without any external stabilizers. The physical properties of synthesized nanoparticles (LM-AgNPs) were characterized using relevant techniques. Formation of silver nanoparticles was demonstrated by visual inspection and by the SPR from UV-VIS absorption. Deploying FESEM and TEM to examine the nanoparticles, the LM-AgNPs were found to have a predominantly spherical to quasi spherical shape. The average size of LM-AgNPs measured from FESEM and TEM was well below 100

nm scale. Thermal decomposition suggested that prepared nanoparticles contain pretty high mass percentages (~97 % Ag) of silver. Stable silver nanoparticles with high metallic content and less amount of phytoconstituents satisfy all the conditions of highly efficient nanoparticles. As anticipated, the prepared LM-AgNPs exhibited significant efficiency for reductive degradation of Congo Red dye. Further we demonstrated the possible application of LM-AgNPs in biomedical field. The LM-AgNPs exhibited potential antibacterial activity suggested that LM-AgNPs might help in the search for novel, successful substitutes to currently available antimicrobial agents. The ability to create stabilized and well-controlled shaped silver nanoparticles through this green approach could have numerous applications in areas such as catalysis, data storage, energy storage, nanomedicine against human and veterinary infections, micro-electronics, and more. It is worth noting that this study contributes to paving the way for more sustainable and economical approaches to synthesizing highly effective silver nanoparticles.

Data availability statement

Data included in article/supp. material/referenced in article.

CRediT authorship contribution statement

Shamsad Sharmin: Formal analysis, Data curation, Investigation, Writing – original draft. **Md Badrul Islam:** Project administration, Supervision. **Barun Kanti Saha:** Project administration, Resources. **Firoz Ahmed:** Software, Validation. **Bijoy Maitra:** Validation, Visualization, Investigation. **M. Zia Uddin Rasel:** Investigation, Validation. **Nazeeb Quaisaar:** Resources, Software. **M. Ahasanur Rabbi:** Conceptualization, Methodology, Project administration, Writing – review & editing.

Declaration of competing interest

The authors declare that they have no known competing financial interests or personal relationships that could have appeared to influence the work reported in this paper.

Acknowledgement

This research is supported by the Bangladesh Council of Scientific and Industrial Research (*Professor Mofizuddin Ahmed Memorial Postgraduate Fellowship*). The authors would like to express their gratitude to the Central Science Laboratory of Rajshahi University for the support it provided to the instrument (TGA). Sincere appreciation was conveyed to the Bangladesh Atomic Energy Commission for their TEM research.

References

- [1] S. Jadoun, R. Arif, N. Kumari, J. Rajesh, K. Meena, Green synthesis of nanoparticles using plant extracts : a review, *Environ. Chem. Lett.* (2020), 0123456789, <https://doi.org/10.1007/s10311-020-01074-x>.
- [2] S. Ahmed, Saifullah, M. Ahmad, B.L. Swami, S. Ikram, Green synthesis of silver nanoparticles using *Azadirachta indica* aqueous leaf extract, *J. Radiat. Res. Appl. Sci.* 9 (1) (2016) 1–7, <https://doi.org/10.1016/j.jrras.2015.06.006>.
- [3] C. Pandit, et al., Journal of king saud university – science biological agents for synthesis of nanoparticles and their applications, *J. King Saud Univ. Sci.* 34 (3) (2022), 101869, <https://doi.org/10.1016/j.jksus.2022.101869>.
- [4] A. Chatterjee, N. Kwatra, J. Abraham, *Nanoparticles Fabrication by Plant Extracts*, 2020, pp. 143–157.
- [5] P. R. Meena Hemlata, A.P. Singh, K.K. Tejavath, Biosynthesis of silver nanoparticles using *cucumis prophetarum* aqueous leaf extract and their antibacterial and antiproliferative activity against cancer cell lines, *ACS Omega* 5 (10) (Mar. 2020) 5520–5528, <https://doi.org/10.1021/acsomega.0c00155>.
- [6] S. Ponarulselvam, C. Panneerselvam, K. Murugan, N. Aarthi, K. Kalimuthu, S. Thangamani, Synthesis of silver nanoparticles using leaves of *Catharanthus roseus* Linn. G. Don and their antiparasitoid activities, *Asian Pac. J. Trop. Biomed.* 2 (7) (2012) 574–580, [https://doi.org/10.1016/S2221-1691\(12\)60100-2](https://doi.org/10.1016/S2221-1691(12)60100-2).
- [7] M. Sharifi-Rad, P. Pohl, F. Epifano, J.M. Álvarez-Suarez, Green synthesis of silver nanoparticles using *astragalus tribuloides delile*. Root extract: characterization, antioxidant, antibacterial, and anti-inflammatory activities, *Nanomaterials* 10 (12) (2020) 1–17, <https://doi.org/10.3390/nano10122383>.
- [8] E.R. Carmona, N. Benito, T. Plaza, G. Recio-Sánchez, Green synthesis of silver nanoparticles by using leaf extracts from the endemic *Buddleja globosa* hope, *Green Chem. Lett. Rev.* 10 (4) (2017) 250–256, <https://doi.org/10.1080/17518253.2017.1360400>.
- [9] H.F. Arintonang, H. Koleangan, A.D. Wuntu, Synthesis of silver nanoparticles using aqueous extract of medicinal plants' (*impatiens balsamina* and *lantana camara*) fresh leaves and analysis of antimicrobial activity, *Internet J. Microbiol.* 2019 (2019), 8642303, <https://doi.org/10.1155/2019/8642303>.
- [10] Y. He, et al., Green synthesis of silver nanoparticles using seed extract of: *alpinia katsumadai*, and their antioxidant, cytotoxicity, and antibacterial activities, *RSC Adv.* 7 (63) (2017) 39842–39851, <https://doi.org/10.1039/c7ra05286c>.
- [11] S. Soares, J. Sousa, A. Pais, C. Vitorino, Nanomedicine: principles, properties, and regulatory issues, *Front. Chem.* 6 (AUG) (2018) 1–15, <https://doi.org/10.3389/fchem.2018.00360>.
- [12] A. Mishra, et al., Green synthesis of silver nanoparticles from leaf extract of *nyctanthes arbor-tristis* L. And assessment of its antioxidant, antimicrobial response, *J. Inorg. Organomet. Polym. Mater.* 30 (2020) 1–13, <https://doi.org/10.1007/s10904-019-01392-w>. Jun.
- [13] P. Roy, B. Das, A. Mohanty, S. Mohapatra, Green synthesis of silver nanoparticles using *Azadirachta indica* leaf extract and its antimicrobial study, 78, *Appl. Nanosci.* 7 (8) (2017) 843–850, <https://doi.org/10.1007/S13204-017-0621-8>. Oct. 2017.
- [14] S. Pirtarighat, M. Ghannadnia, S. Baghshahi, Green synthesis of silver nanoparticles using the plant extract of *Salvia spinosa* grown in vitro and their antibacterial activity assessment, *J. Nanostructure Chem.* 9 (1) (2019) 1–9, <https://doi.org/10.1007/s40097-018-0291-4>.
- [15] M.M.I. Masum, et al., Biogenic synthesis of silver nanoparticles using *Phyllanthus emblica* fruit extract and its inhibitory action against the pathogen *acidovorax oryzae* strain RS-2 of rice bacterial Brown stripe, *Front. Microbiol.* 10 (2019) 820, <https://doi.org/10.3389/fmicb.2019.00820>.
- [16] S. Shabina, S. Gaurav, A.M. Irfan, M. Sarmad, *Green nanotechnology: a review on nanomedicinal potential and green synthesis of silver nanoparticles (ag-np's)*, *Res. J. Biotechnol.* 15 (10) (2020) 177–187.
- [17] L. Castillo-Henríquez, K. Alfaro-Aguilar, J. Ugalde-Álvarez, L. Vega-Fernández, G. Montes de Oca-Vásquez, J.R. Vega-Baudrit, Green synthesis of gold and silver nanoparticles from plant extracts and their possible applications as antimicrobial agents in the agricultural area, *Nanomaterials* 10 (9) (2020), <https://doi.org/10.3390/nano10091763>. Sep.

- [18] A.K. Keshari, R. Srivastava, P. Singh, V.B. Yadav, G. Nath, Antioxidant and antibacterial activity of silver nanoparticles synthesized by *Cestrum nocturnum*, *J. Ayurveda Integr. Med.* 11 (1) (2020) 37–44, <https://doi.org/10.1016/j.jaim.2017.11.003>.
- [19] N. Krithiga, A. Rajalakshmi, A. Jayachitra, Green Synthesis of Silver Nanoparticles Using Leaf Extracts of *Clitoria ternatea* and *Solanum nigrum* and Study of Its Antibacterial Effect against Common Nosocomial Pathogens, *J. Nanosci.* 2015 (2015) 1–8, <https://doi.org/10.1155/2015/928204>.
- [20] Z. Bedlovičová, A. Salayová, Green-synthesized Silver Nanoparticles and Their Potential for Antibacterial Applications, 2023.
- [21] M. Islam, M. Sarkar, M. Shafique, M. Jalil, M. Haque, R. Amin, Phytochemical screening and anti-microbial activity studies on *Leea macrophylla* seed extracts, *J. Sci. Res.* 5 (May 2013), <https://doi.org/10.3329/jsr.v5i2.13213>.
- [22] S. Akhter, M.A. Rahman, J. Aklima, M.R. Hasan, J.M.K. Hasan Chowdhury, Antioxidative role of hatikana (*Leea macrophylla* roxb.) partially improves the hepatic damage induced by CCl4 in wistar albino rats, *BioMed Res. Int.* 2015 (2015), <https://doi.org/10.1155/2015/356729>.
- [23] R. Bin Rashid, R. Kuddus, M.A. Rashid, Original Article Pharmacological and phytochemical screenings of ethanol extract of *Leea macrophylla* Roxb, *Innov. Pharm. Pharmacother.* 2 (1) (2014) 321–327.
- [24] A. Joshi, D.S. Prasad, V. Joshi, S. Hemalatha, Phytochemical standardization, antioxidant, and antibacterial evaluations of *Leea macrophylla*: a wild edible plant, *J. Food Drug Anal.* 24 (Jan) (2016), <https://doi.org/10.1016/j.jfda.2015.10.010>.
- [25] M. Roxb, "Mahmud et al.," vol. 2, no. 12, pp.3230–3234, 2011..
- [26] Z. Al Mahmud, et al., Phytochemical investigations and antioxidant potential of roots of *Leea macrophylla* (Roxb), *BMC Res. Notes* (2017) 1–9, <https://doi.org/10.1186/s13104-017-2503-2>.
- [27] J. Mawa, A. Rahman, M.A. Hashem, J. Hosen, *Leea macrophylla* root extract upregulates the mRNA expression for antioxidative enzymes and repairs the necrosis of pancreatic β -cell and kidney tissues in fructose-fed Type 2 diab ... *Biomedicine & Pharmacotherapy* *Leea macrophylla* root extract upregulat," *Biomed. Pharmacother* 110 (November) (2018) 74–84, <https://doi.org/10.1016/j.biopha.2018.11.033>.
- [28] D. Sarvade, R. Acharya, *Leea Macrophylla* Roxb. Ex Hornem.: an Ethnomedicinal, Ethnic Food, Economical, and Pharmacological Update, March, 2019.
- [29] M.K. Hossain, H. Minami, S.M. Hoque, M.M. Rahman, M.K. Sharafat, M.F. Begum, M.E. Islam, H. Ahmad, Mesoporous electromagnetic composite particles: electric current responsive release of biologically active molecules and antibacterial properties, *Colloids Surf., B* 181 (2019) 85–93, <https://doi.org/10.1016/j.colsurfb.2019.05.040>.
- [30] J.L. Rios, M.C. Recio, A. Villar, Screening methods for natural products with antimicrobial activity: a review of the literature, *J. Ethnopharmacol.* 23 (2–3) (1988) 127–149, [https://doi.org/10.1016/0378-8741\(88\)90001-3](https://doi.org/10.1016/0378-8741(88)90001-3).
- [31] B.N. Meyer, N.A. Ferrigni, J.E. Putnam, L.B. Jacobsen, D.E. Nichols, J.L. Mclaughlin, Brine Shrimp : A Convenient General Bioassay for Active Plant Constituents 45 (1982) 31–34.
- [32] C. Arulvasu, S.M. Jennifer, D. Prabhu, D. Chandhirasekar, Toxicity effect of silver nanoparticles in brine shrimp artemia, *Sci. World J.* 2014 (2014), <https://doi.org/10.1155/2014/256919>.
- [33] S.A. Al-Thabaiti, A.Y. Obaid, S. Hussain, Z. Khan, Shape-directing role of cetyltrimethylammonium bromide on the morphology of extracellular synthesis of silver nanoparticles, *Arab. J. Chem.* 8 (4) (2015) 538–544, <https://doi.org/10.1016/j.arabjc.2014.11.030>.
- [34] J. Jana, M. Ganguly, T. Pal, Enlightening surface plasmon resonance effect of metal nanoparticles for practical spectroscopic application, *RSC Adv.* 6 (Jan) (2016), <https://doi.org/10.1039/C6RA14173K>.
- [35] D. Sarathi Kannan, S. Mahboob, K.A. Al-Ghanim, P. Venkatachalam, Antibacterial, antibiofilm and photocatalytic activities of biogenic silver nanoparticles from *ludwigia octovalvis*, *J. Cluster Sci.* 32 (2) (Mar. 2021) 255–264, <https://doi.org/10.1007/s10876-020-01784-w>.
- [36] S.V. Kumar, A.P. Bafana, P. Pawar, A. Rahman, S.A. Dahoumane, C.S. Jeffryes, High conversion synthesis of <10 nm starch-stabilized silver nanoparticles using microwave technology, *Sci. Rep.* 8 (1) (2018), <https://doi.org/10.1038/s41598-018-23480-6>. Dec.
- [37] S.E. Agarry, C.N. Owabor, A.O. Ajani, Modified plantain peel as cellulose-based low-cost adsorbent for the removal of 2,6-DICHLOROPHENOL from aqueous solution: adsorption isotherms, kinetic modeling, and thermodynamic studies, *Chem. Eng. Commun.* 200 (8) (Aug. 2013) 1121–1147, <https://doi.org/10.1080/00986445.2012.740534>.
- [38] J.R. Carney, A. V Fedorov, J.R. Cable, T.S. Zwier, Infrared spectroscopy of H-bonded bridges stretched across the cis-amide group: I. Water bridges, *J. Phys. Chem. A* 105 (14) (Apr. 2001) 3487–3497, <https://doi.org/10.1021/jp003375f>.
- [39] S.E. Agarry, K.M. Oghenejoboh, O.A. Aworanti, A.O. Arinkoola, Biocorrosion inhibition of mild steel in crude oil-water environment using extracts of *Musa paradisiaca* peels, *Moringa oleifera* leaves, and *Carica papaya* peels as biocidal-green inhibitors: kinetics and adsorption studies, *Chem. Eng. Commun.* 206 (1) (Jan. 2019) 98–124, <https://doi.org/10.1080/00986445.2018.1476855>.
- [40] J.L. Mortensen, D.M. Anderson, J.L. White, Infrared Spectrometry," *Methods Of Soil Analysis, Part 1: Physical And Mineralogical Properties, Including Statistics Of Measurement And Sampling*, 2015, pp. 743–770, <https://doi.org/10.2134/agronmonogr9.1.c51>.
- [41] N.N. Bonnia, M.S. Kamaruddin, M.H. Nawawi, S. Ratim, H.N. Azlina, E.S. Ali, Green biosynthesis of silver nanoparticles using 'polygonum hydropiper' and study its catalytic degradation of methylene blue, *Procedia Chem.* 19 (2016) 594–602, <https://doi.org/10.1016/j.proche.2016.03.058>.
- [42] V.K. Rokhade, T. Taranath, PHYTOSYNTHESIS of silver nanoparticles using fruit extract of leea indica (burm. F.) merr. And their antimicrobial property, *Int. J. Pharma Sci. Res.* 8 (3) (2017) 1319–1325, [https://doi.org/10.13040/IJPSR.0975-8232.8\(3\).1319-25](https://doi.org/10.13040/IJPSR.0975-8232.8(3).1319-25).
- [43] T.Y. Suman, S.R. Radhika Rajasree, A. Kanchana, S.B. Elizabeth, Biosynthesis, characterization and cytotoxic effect of plant mediated silver nanoparticles using *Morinda citrifolia* root extract, *Colloids Surf., B* 106 (Jun. 2013) 74–78, <https://doi.org/10.1016/j.colsurfb.2013.01.037>.
- [44] P. Manimaran, S.P. Saravanan, M.R. Sanjay, S. Siengchin, M. Jawaid, A. Khan, Characterization of new cellulose fiber: *dracaena reflexa* as a reinforcement for polymer composite structures, *J. Mater. Res. Technol.* 8 (2) (2019) 1952–1963, <https://doi.org/10.1016/j.jmrt.2018.12.015>.
- [45] S. Raiyan, et al., Natural compounds from *Leea macrophylla* enhance phagocytosis and promote osteoblasts differentiation by alkaline phosphatase, type 1 collagen, and osteocalcin gene expression, *J. Biomed. Mater. Res., Part A* 109 (7) (2021) 1113–1124, <https://doi.org/10.1002/jbm.a.37103>. Jul.
- [46] P. Moteriyya, S. Chanda, Biosynthesis of silver nanoparticles formation from *Caesalpinia pulcherrima* stem metabolites and their broad spectrum biological activities, *J. Genet. Eng. Biotechnol.* 16 (1) (2018) 105–113, <https://doi.org/10.1016/j.jgeb.2017.12.003>.
- [47] A.K. Mittal, J. Bhaumik, S. Kumar, U.C. Banerjee, Biosynthesis of silver nanoparticles: elucidation of prospective mechanism and therapeutic potential, *J. Colloid Interface Sci.* 415 (Feb. 2014) 39–47, <https://doi.org/10.1016/j.jcis.2013.10.018>.
- [48] B. Maitra, et al., Biosynthesis of *Bixa orellana* seed extract mediated silver nanoparticles with moderate antioxidant, antibacterial and antiproliferative activity, *Arab. J. Chem.* 16 (5) (2023), 104675, <https://doi.org/10.1016/j.arabjc.2023.104675>.
- [49] P. Karthiga, Preparation of silver nanoparticles by *Garcinia mangostana* stem extract and investigation of the antimicrobial properties, *Biotechnol. Res. Innov.* 2 (1) (2018) 30–36, <https://doi.org/10.1016/j.biori.2017.11.001>.
- [50] M.A. Rabbi, M.M. Rahman, H. Minami, M.R. Habib, H. Ahmad, Ag impregnated sub-micrometer crystalline jute cellulose particles: catalytic and antibacterial properties, *Carbohydr. Polym.* 233 (2020), <https://doi.org/10.1016/j.carbpol.2020.115842>. Apr.
- [51] J. Lim, S.P. Yeap, H.X. Che, S.C. Low, Characterization of magnetic nanoparticle by dynamic light scattering, *Nanoscale Res. Lett.* 8 (1) (2013) 381, <https://doi.org/10.1186/1556-276X-8-381>.
- [52] X.-F. Zhang, Z.-G. Liu, W. Shen, S. Gurunathan, Silver nanoparticles: synthesis, characterization, properties, applications, and therapeutic approaches, *Int. J. Mol. Sci.* 17 (9) (2016), <https://doi.org/10.3390/ijms17091534>.
- [53] B. Adebayo-Tayo, A. Salaam, A. Ajibade, Green synthesis of silver nanoparticle using *Oscillatoria* sp. extract, its antibacterial, antibiofilm potential and cytotoxicity activity, *Heliyon* 5 (2019), e02502, <https://doi.org/10.1016/j.heliyon.2019.e02502>.
- [54] L.M. Liz-Marzán, M. Giersig, P. Mulvaney, Synthesis of nanosized gold-silica core-shell particles, *Langmuir* 12 (18) (1996) 4329–4335, <https://doi.org/10.1021/la9601871>.
- [55] K. Kartini, A. Alviani, D. Anjarwati, A.F. Fanany, J. Sukweenadhi, C. Avanti, Process optimization for green synthesis of silver nanoparticles using Indonesian medicinal plant extracts, *Processes* 8 (8) (2020), <https://doi.org/10.3390/pr8080998>.
- [56] S. Kaviya, J. Santhanalakshmi, B. Viswanathan, J. Muthumary, K. Srinivasan, Biosynthesis of silver nanoparticles using citrus sinensis peel extract and its antibacterial activity, *Spectrochim. Acta. A. Mol. Biomol. Spectrosc.* 79 (3) (Aug. 2011) 594–598, <https://doi.org/10.1016/j.saa.2011.03.040>.

- [57] Y.Y. Loo, et al., In Vitro Antimicrobial Activity of Green Synthesized Silver Nanoparticles Against Selected Gram-negative Foodborne Pathogens," *Front. Microbiol.* 9 (2018), <https://doi.org/10.3389/fmicb.2018.01555>.
- [58] G.M. Raghavendra, T. Jayaramudu, K. Varaprasad, G.S. Mohan Reddy, K.M. Raju, Antibacterial nanocomposite hydrogels for superior biomedical applications: a Facile eco-friendly approach, *RSC Adv.* 5 (19) (2015) 14351–14358, <https://doi.org/10.1039/c4ra15995k>.
- [59] S. Chavan, V. Nandanathangam, Shifts in metabolic patterns of soil bacterial communities on exposure to metal engineered nanomaterials, *Ecotoxicol. Environ. Saf.* 189 (2020), 110012, <https://doi.org/10.1016/j.ecoenv.2019.110012>.
- [60] S.H. Nam, et al., Conducting a battery of bioassays for gold nanoparticles to derive guideline value for the protection of aquatic ecosystems, *Nanotoxicology* 9 (3) (2015) 326–335, <https://doi.org/10.3109/17435390.2014.930531>.
- [61] N. Hamrun, T. Nabilah, R. Hasyim, M. Ruslin, I. Dammar, M.A.A. Arianto, Toxicity test of bioactive red alga extract *eucheuma spinosum* on shrimp *Artemia salina* leach, *Sys. Rev. Pharm.* 11 (2020) 672–676.
- [62] N. Nerdy, et al., Brine shrimp (*Artemia salina* leach.) lethality test of ethanolic extract from green betel (piper betle linn.) and red betel (piper crocatum ruiz and pav.) through the soxhletation method for cytotoxicity test, *Open Access Maced. J. Med. Sci.* 9 (2021) 407–412, <https://doi.org/10.3889/oamjms.2021.6171>. May.
- [63] P.N. Solis, C.W. Wright, M.M. Anderson, M. Gupta, A Microwell Cytotoxicity Assay using *Artemia Sauna* (Brine Shrimp), 1992, pp. 250–252.
- [64] R.T. 2nd Trotter, M.H. Logan, J.M. Rocha, J.L. Boneta, Ethnography and bioassay: combined methods for a preliminary screen of home remedies for potential pharmacological activity, *J. Ethnopharmacol.* 8 (1) (1983) 113–119, [https://doi.org/10.1016/0378-8741\(83\)90092-2](https://doi.org/10.1016/0378-8741(83)90092-2). Jul.
- [65] P. Mayorga, K. Pérez, S. Cruz, A. Caceres, Comparison of bioassays using the anostracan crustaceans *Artemia salina* and *Thamnocephalus platyurus* for plant extract toxicity screening, *Rev. Bras. Farmacogn.* 20 (Oct. 2010) 897–903, <https://doi.org/10.1590/S0102-695X2010005000029>.
- [66] R. Rekulapally, L.N.M. Chavali, M.M. Idris, S. Singh, Toxicity of TiO₂, SiO₂, ZnO, CuO, Au and Ag engineered nanoparticles on hatching and early nauplii of *Artemia* sp, *PeerJ* 1 (2019) 2019, <https://doi.org/10.7717/peerj.6138>.
- [67] P. Kumar, et al., Antibacterial activity and in-vitro cytotoxicity assay against brine shrimp using silver nanoparticles synthesized from *Sargassum ilicifolium*, *Dig. J. Nanomater. Biostruct.* 7 (4) (2012) 1447–1455.
- [68] M. Rabbi, J. Hossen, M. Sarwar, P. Roy, S. Binte Shaheed, M. Hasan, Investigation of waste water quality parameters discharged from textile manufacturing industries of Bangladesh, *Curr. World Environ.* 13 (Aug. 2018) 206–214, <https://doi.org/10.12944/CWE.13.2.05>.
- [69] K. Jyoti, A. Singh, Green synthesis of nanostructured silver particles and their catalytic application in dye degradation, *J. Genet. Eng. Biotechnol.* 14 (2) (2016) 311–317, <https://doi.org/10.1016/j.jgeb.2016.09.005>.